Original Article

Development, evaluation and optimization of superparamagnetite nanoparticles prepared by co-precipitation method

Hashem Montaseri*, Shohreh Alipour, and Molood Alsadat Vakilinezhad

Quality control Department, Faculty of Pharmacy, Shiraz University of Medical Sciences, Shiraz, I.R. Iran.

Abstract

Magnetic nanoparticles (MNPs) are of high interest due to their application in medical fields, in particular for theranostics. Specific properties required for such particles include high magnetization, appropriate size and stability. Biocompatible magnetically soft magnetite particles (Fe_3O_4) have been investigated for biological purposes. The intrinsic instability of these nanoparticles and their susceptibility to the oxidization in air, are limitations for their applications. Various methods have been described for synthesis of these nanoparticles among which co-precipitation method is widely experimented. In order to illustrate the synthesis of MNPs elaborately, the effect of different factors on particle formation were studied. The particles morphology, stability, paramagnetic effect, chemical structure and cytotoxicity were evaluated. Particles of 58 and 60 nm obtained by oleic acid coated (OMNPs) and citric acid coated (CMNPs) magnetite nanoparticles respectively. Transmission electron microscopy images exhibited the real sizes are 15 and 13 nm. Magnetic saturations of these nanoparticles were 72 and 68 emu/g which is suitable for medical applications. Both OMNPs and CMNPs were non-toxic to the SK-Br-3 and MCF-7 cells in the concentrations of <2.5 μg/mL. Since these particles exhibit relatively high magnetic saturation, low dose of such material would be required; therefore, these NPs seem to be suitable for theranostics.

Keywords: Magnetic nanoparticles; Oleic acid; Citric acid; SK-Br-3; MCF-7

INTRODUCTION

Magnetic nanoparticles (MNPs) are of high interest due to their various applications including serving as carrier in controlled drug delivery, theranostics, hyperthermia treatment, and contrast enhancement agent. Besides the first known magnetic material, Fe_3O_4, many other substances show magnetic properties. Various magnetic materials are chosen based on their desired effects (1-3).

In order to exhibit superparamagnetic behavior, the size of MNPs should be smaller than their critical value, which defined as the energy needed to maintain and support the magnetic field of single domain particles in relation to the external magnetic source. These MNPs not only show superparamagnetism, but also resist precipitation, have large constant magnetic moment, have negligible remanence and coercivity with no hysteresis in the magnetization curve and do not stay magnetized for an extended period of time.

Being biocompatible, besides all these specifications, these MNPs considered suitable for drug delivery (4-6).

Multiple researchers attempted to synthesize monodispersed and stable MNPs with well-defined shapes. A pragmatic approach to synthesize iron oxide MNPs is co-precipitation technic. Co-precipitation often results in MNPs of amenable sizes for drug delivery with reproducible outcomes. In this method, iron salts are precipitated as a magnetite in the alkaline media. The type of iron salts (i.e. chlorides, sulfates, or nitrates), Fe^{2+} to Fe^{3+} ratios, reaction temperature and ionic strength of the media are the important parameters that affect MNPs composition and morphology (5,7). The major challenge in production of MNPs is to form particles of sizes below the critical value that remain stable over longer periods of time.

*Corresponding author: H. Montaseri
Tel: +98-9177111029, Fax: +98-7132425403
Email: Hmontase@sums.ac.ir

As the particle size decreases, the surface area and thereby the surface energy increases, which enhances the chance of particle aggregation (4). Moreover, highly active naked metallic particles are easily oxidized in air that reduces magnetism of the MNPs. The smaller the MNPs, the more susceptible they are toward oxidation (7). Therefore, producing chemically stable magnetic nanoparticles are essential for many applications such as protein and cell separation and magnetofection (8-9). Developing efficient techniques that improve the chemical stability of magnetic nanoparticles is crucial. Since the naked MNPs would rapidly aggregate, an effective coating to reduce the aggregation is essential.

Herein, we aimed to prepare, characterize and surface coat MNPs to engineer particles for theranostics. The effect of different processing and formulation variables on particle size and size distribution of MNPs were investigated. This leads to production of optimum MNPs with high magnetic properties, appropriate size and stability.

MATERIALS AND METHODS

Materials

Synthetic materials including iron (II) chloride tetrahydrate ($FeCl_2.4H_2O$), iron (III) chloride hexahydrate ($FeCl_3.6H_2O$), ammonium hydroxide (NH_4OH), oleic acid, Span® 80 and Tween® 80 were purchased in analytical grade from Merck, Germany. Required solvents such as acetonitrile and dichrolomethan were provided from Merck, Germany. Polyvinyl alcohol (MW~72000; 97.5-99.5 mol% hydrolysis), citric acid (monohydrate) and carboxymethyl cellulose were purchased from Fluka, Switzerland. Cell lines were provided by Pasteur Institute, Iran. Essential cell culture media components, RPMI 1640 and fetal bovine serum (FBS) were purchased from Biosera, UK. 3-(4,5-dimethylthiazol-2-yl)-2,5-diphenyltetra-zolium bromide (MTT) was procured from Sigma, USA.

Preparation of MNPs

MNPs were prepared by co-precipitation of the aqueous iron salts in alkaline media under inert nitrogen purge (10). Different volumes of 0.1 M $FeCl_3.6H_2O$ and 0.1 M $FeCl_2.4H_2O$ solutions in deoxygenated water were mixed in a three-necked round flask to obtain the iron salts ratio ($FeCl_3:FeCl_2$) of 1.5 or 2 or 2.5. The temperature was raised to 70 ± 5 °C. Ammonium hydroxide (7 mL, 25% W/W) was added to adjust the pH to 9. Upon pH changes, black magnetite crystals were formed. Oleic acid (OA, 1g, 0.7 mM) was added dropwise as the stabilizing agents. Temperature was increased to 110 ± 5 °C to evaporate the excess water. MNPs were separated with magnetic decantation. Collected MNPs were washed three times with distilled water and ethanol. The effect of iron salts ratio, mixing method and mixing duration on particle size and size distribution were evaluated. All formulations were prepared in triplicate. Under these circumstances 27 formulations were prepared and evaluated in terms of mean particle size and SPAN values. The optimized formulation (OMNPs-17) in this stage was selected for further investigation to evaluate the effect of mixing intensity, alkalinizing agent type and its addition speed, concentration of OA and drying method on particle size in five various stages. The best formulation (OMNPs-37) at this point was chosen for further optimization of different stabilizers. This formulation was used to evaluate the effect of different stabilizing agents such as polyvinyl alcohol (PVA, 1%), carboxymethyl cellulose (CMC, 1%) and citric acid (CA, 1.6 mM) on particle size and size distribution of MNPs.

Characterization of hydrophobic magnetite nanoparticles
Size of MNPs

The particle size and polydispersity index of MNPs were measured using laser diffraction technique (Shimadzu SALD-2101, Japan). Volume-based diameter of MNPs were measured. Dispersity of nanoparticles was calculated by SPAN value using following equation:

$$SPAN = \frac{d(0.9) - d(0.1)}{d(0.5)}$$

Morphology of MNPs

The MNPs with the smallest size were selected and their morphology was evaluated by transmission electron microscopy (TEM, Philips-CM10, Holland). Samples were

embedded in epoxy resin, placed on carbon film coated copper grid and imaged.

Stability of MNPs

Naked MNPs were rapidly precipitated because of their surface charge. In order to find the proper coating for MNPs, 1 mg of coated MNPs were dispersed in 5 mL of hexane and their stability were studied for 24 h. Particles which precipitate at slower rate was considered stable.

Magnetic properties of MNPs

Alternating field gradient magnetometer (AFGM-MDK, Iran) was used to evaluate the magnetic properties of the fabricated MNPs. Samples were fitted between the pole pieces of the magnet. Magnetic field was increased to 10,000 Oe and then reversed so that sample hysteresis curve was obtained.

Chemical structure of MNPs

The MNPs chemical structure and crystallinity was determined by X-ray powder diffraction (XRPD-Philips, Holland). The scans were conducted at the range of 2θ from 20 to 90º. The resulting diffraction pattern was compared with library data of magnetite.

MNPs interaction with coating material

To investigate the possible interaction between MNPs and coating materials, the Fourier transform infrared (FTIR) spectroscopy method were used. The spectra were taken in the range of 400-4000 cm^{-1}.

In vitro cell viability assay for MNPs

Dose-response curves utilizing two breast cancer cell lines, SK-BR-3 and MCF-7, were constructed. Cells were seeded at 5,000 cells per well in RPMI supplemented with 10% FBS and incubated for 48 h to allow cell attachment. MNPs suspensions in culture media (150 µL of 10 to 0.31 µg/mL) were replaced with each well content. For each concentration, three plates were prepared and all experiments were performed in triplicate. Plates were then incubated for 24, 48 or 72 h. At the specified time intervals, the content of each well was replaced with 150 µL media containing MTT (5 mg/mL) and plates were

incubated for another 4 h. Then MTT solution was replaced with 150 µL of DMSO to lyse cells and dissolve formazan crystals. Microplate reader (Anthos 2020, USA) was used to measure absorption at 492 nm. Control cells assuming to have 100% viability were remained untreated (11).

Data analysis and statistics

For statistical analysis, ANOVA with the Tukey Post Hoc test were performed using SPSS® statistics 17.0 (windows-based version). Origin (8.0) software was employed to plot the data.

RESULTS

Preparation and optimization of MNPs

To evaluate the variables affecting MNPs size and size distribution, various parameters were examined. The smallest particles with the range of 70 nm were obtained with iron salts ratio of 2 and 2.5 and mixing time of 30 min via probe sonication (Table 1). The particle size of these two formulations, OMNPs-17 and OMNPs-26, did not show statistically significant differences.

However, since OMNPs-17 size distribution exhibited a unimodal pattern compared to OMNPs-26, it was adopted as the optimized formulation. Further optimization of the method produced nanoparticles of 58 nm with the narrowest distribution by probe sonication intensity of 100%, rapid addition of ammonia as the base, use of OA at concentration of 0.2 mg/mL, and freeze drying technic (Table 2). Table 3 shows the effect of different stabilizing agents including OA, PVA, CA and CMC on particle size and size distribution of MNPs. OMNPs-37 and CMNPs-39 formulations with particle sizes of 58 and 60 nm were considered most appropriate.

Characterization of MNPs
Morphology of MNPs

TEM images of the smallest naked MNPs, OMNPs and CMNPs are shown in Fig. 1. TEM of naked MNPs shows particles aggregation. Particle size of OMNPs and CMNPs were 15 nm and 13 nm respectively.

Table 1. Impact of salt ratio, mixing method and time on particle size and size distribution of magnetic nanoparticles.

Formulation	Fe^{3+}/Fe^{2+}	Mixing method	Mixing time (min)	Mean volume (nm)	SPAN
OMNPs-1	1.5	Magnetic stirrer	15	13710 ± 12.14	4.70 ± 4.05
OMNPs-2	1.5	Magnetic stirrer	30	10880 ± 3.21	4.53 ± 21.92
OMNPs-3	1.5	Magnetic stirrer	45	18240 ± 5.30	4.49 ± 10.14
OMNPs-4	1.5	Bath sonication	15	32660 ± 58.62	3.04 ± 8.72
OMNPs-5	1.5	Bath sonication	30	11040 ± 0.65	4.03 ± 0.75
OMNPs-6	1.5	Bath sonication	45	8010 ± 4.72	2.89 ± 16.71
OMNPs-7	1.5	Probe sonication	15	11630 ± 4.06	5.18 ± 1.90
OMNPs-8	1.5	Probe sonication	30	8510 ± 3.35	2.35 ± 2.56
OMNPs-9	1.5	Probe sonication	45	2480 ± 0.92	3.08 ± 9.33
OMNPs-10	2	Magnetic stirrer	15	1800 ± 1.30	2.66 ± 1.17
OMNPs-11	2	Magnetic stirrer	30	6720 ± 4.63	2.41 ± 1.93
OMNPs-12	2	Magnetic stirrer	45	2310 ± 2.41	1.57 ± 12.44
OMNPs-13	2	Bath sonication	15	27090 ± 26.92	2.71 ± 5.11
OMNPs-14	2	Bath sonication	30	7270 ± 5.68	2.64 ± 5.57
OMNPs-15	2	Bath sonication	45	20480 ± 23.25	2.34 ± 10.83
OMNPs-16	2	Probe sonication	15	1010 ± 1.44	4.13 ± 8.80
OMNPs-17	**2**	**Probe sonication**	**30**	**70 ± 0.32**	**0.81 ± 0.56**
OMNPs-18	2	Probe sonication	45	80 ± 0.84	0.81 ± 1.52
OMNPs-19	2.5	Magnetic stirrer	15	15780 ± 5.47	2.23 ± 4.15
OMNPs-20	2.5	Magnetic stirrer	30	11730 ± 3.49	3.42 ± 9.21
OMNPs-21	2.5	Magnetic stirrer	45	1590 ± 0.65	2.28 ± 1.20
OMNPs-22	2.5	Bath sonication	15	13490 ± 3.56	3.14 ± 8.31
OMNPs-23	2.5	Bath sonication	30	8660 ± 5.48	2.24 ± 1.96
OMNPs-24	2.5	Bath sonication	45	7910 ± 3.75	3.85 ± 3.22
OMNPs-25	2.5	Probe sonication	15	103 ± 0.44	0.66 ± 15.18
OMNPs-26	2.5	Probe sonication	30	70 ± 1.93	0.76 ± 0.84
OMNPs-27	2.5	Probe sonication	45	82 ± 2.10	1.064 ± 6.93

OMNPs, oleic acid coated magnetite nanoparticles.

Table 2. Impact of mixing intensity, alkalizing agent and its addition time, concentration of stabilizers and drying method on particle size and size distribution of magnetic nanoparticles.

Formulation[A]	Mixing intensity	Alkalizing agent	Ammonia addition time	OA conc	Drying method	Mean volume (nm)	SPAN
OMNPs-17	100%	NH_4OH	Rapidly	0.2	Magnetic decant	70 ± 0.32	0.81 ± 0.56
OMNPs-28	60%	NH_4OH	Rapidly	0.2	Magnetic decant	12500 ± 26.4	2.99 ± 26.93
OMNPs-29	80%	NH_4OH	Rapidly	0.2	Magnetic decant	1330 ± 0.83	3.95 ± 32.70
OMNPs-17	100%	NH_4OH	Rapidly	0.2	Magnetic decant	70 ± 0.32	0.81 ± 0.56
OMNPs-30	100%	KOH	Rapidly	0.2	Magnetic decant	360 ± 0.48	0.78 ± 0.41
OMNPs-31	100%	NaOH	Rapidly	0.2	Magnetic decant	750 ± 0.44	2.49 ± 10.15
OMNPs-17	100%	NH_4OH	Rapidly	0.2	Magnetic decant	70 ± 0.32	0.81 ± 0.56
OMNPs-32	100%	NH_4OH	1 min	0.2	Magnetic decant	1370 ± 3.06	1.22 ± 12.17
OMNPs-33	100%	NH_4OH	5 min	0.2	Magnetic decant	5100 ± 2.37	1.79 ± 1.63
OMNPs-17	100%	NH_4OH	Rapidly	0.2	Magnetic decant	70 ± 0.32	0.81 ± 0.56
OMNPs-34	100%	NH_4OH	Rapidly	0.4	Magnetic decant	87 ± 0.18	2.62 ± 12.94
OMNPs-35	100%	NH_4OH	Rapidly	0.8	Magnetic decant	100 ± 0.14	1.77 ± 22.50
OMNPs-17	100%	NH_4OH	Rapidly	0.2	Magnetic decant	70 ± 0.32	0.81 ± 0.56
OMNPs-36	100%	NH_4OH	Rapidly	0.2	Rotary evaporate	87 ± 0.51	3.64 ± 17.52
OMNPs-37	**100%**	**NH_4OH**	**Rapidly**	**0.2**	**Freeze dry**	**58 ± 0.18**	**0.53 ± 0.16**

A, the constant situations are: Fe^{3+}/Fe^{2+} ratio = 2; mixing method = probe sonication; time of mixing = 30 min; OA conc, oleic acid concentration; OMNPs, oleic acid coated magnetite nanoparticles.

Stability of MNPs

Evaluations of OMNPs and CMNPs stabilities in hexane showed no precipitation within 24 h. Lack of precipitation resulted from sufficient coating by OA or CA. However, after 2 weeks the height of precipitate reached to about 1 and 1.7 mm for OMNPs and CMNPs respectively.

Table 3. Effect of different stabilizing agents on particle size and size distribution of magnetic nanoparticles.

Formulation	Stabilizing agent	Mean volume (nm)	SPAN
OMNPs-37	OA	**58 ± 0.18**	**0.53 ± 0.16**
MNPs-38	PVA	79 ± 8.05	0.69 ± 3.11
CMNPs-39	CA	**60 ± 0.24**	**0.49 ± 0.29**
MNPs-40	CMC	89 ± 4.33	1.05 ± 0.70

OA, oleic acid; PVA, polyvinyl alcohol; CA, citric acid; CMC, carboxymethyl celloluse; MNPs, magnetite nanoparticles; OMNPs, oleic acid-coated magnetite nanoparticles; CMNPs, citric acid-coated magnetite nanoparticles
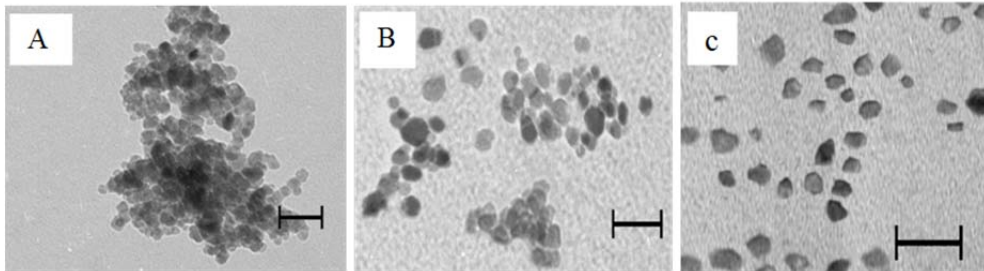
Fig. 1. Transmission electron microscopic images of magnetite nanoparticles (bar scale indicates 20 nm); (A) naked magnetite nanoparticles, (B) oleic acid coated magnetite nanoparticles, and (C) citric acid coated magnetite nanoparticles.
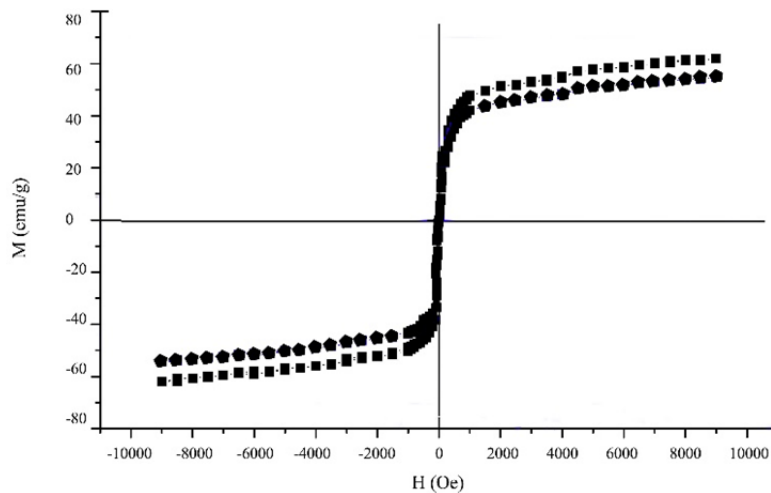
Fig. 2. Magnetization curves of oleic acid-coated magnetite nanoparticles (square line), and citric acid coated magnetite nanoparticles (pentagon line).
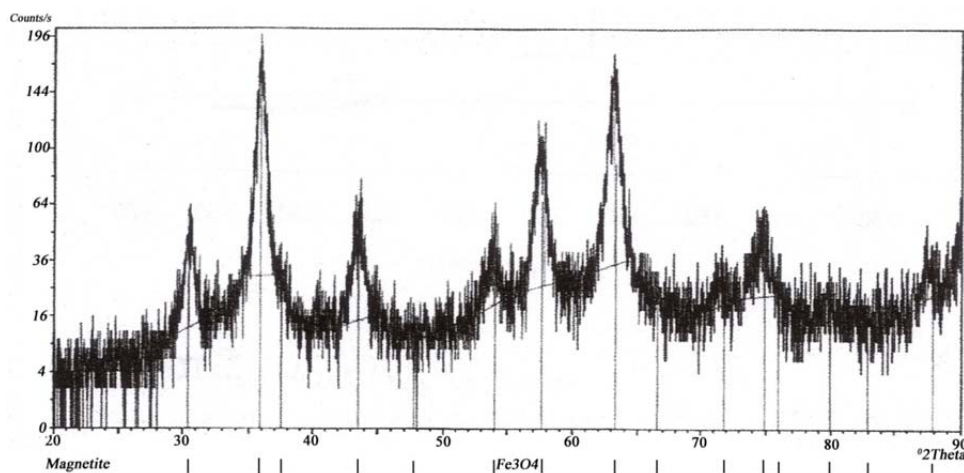
Fig. 3. *X-ray powder diffraction* of synthesized magnetite nanoparticles.

278

Magnetic properties of MNPs

Magnetization curves of OMNPs and CMNPs are depicted in Fig. 2. Increase and decrease in magnetization curves are almost conforming of paramagnetic materials (4). According to this histogram, the selected OMNPs and CMNPs showed magnetic saturation of about 72 and 68 emu/g with little reminence time.

Chemical structure of MNPs

X-ray powder diffraction of resulting MNPs characterized with XRPD is shown in Fig. 3. Characteristic peaks of magnetite are detected at $2\theta = 30.1º, 35.5º, 43.1º, 53.4º, 57.0º$ and $62.6º$.

MNPs interaction with coating material

FTIR spectrums of the MNPs, OA, OMNPs, CA and CMNPs are illustrated in Fig. 4. Fe–O vibration of magnetite particles at 580-590 cm^{-1}, carboxyl vibration of OA carboxyl group at 1630 cm^{-1} and elimination of carboxyl vibration of citric acid at 1780 cm^{-1} is observed in these spectra.

***In vitro* cell viability assay for MNPs**

The cytotoxicity of OMNPs-37 and CMNPs-39 were investigated. Data show that at concentrations < 2.5 µg/mL cytotoxicity is minimal.

MNPs are usually used at lower concentrations for drug delivery (12). Results are shown in Fig. 5. Approximate IC$_{50}$ of OMNPs-37 was 4.8 ± 0.9 µg/mL for SK-Br-3 and 4 ± 1.6 µg/mL for MCF-7 cells. Approximate IC$_{50}$ of CMNPs-39 was 4.5 ± 1.4 µg/mL and 3.6 ± 0.8 µg/mL for SK-Br-3 and MCF-7 cells, respectively.
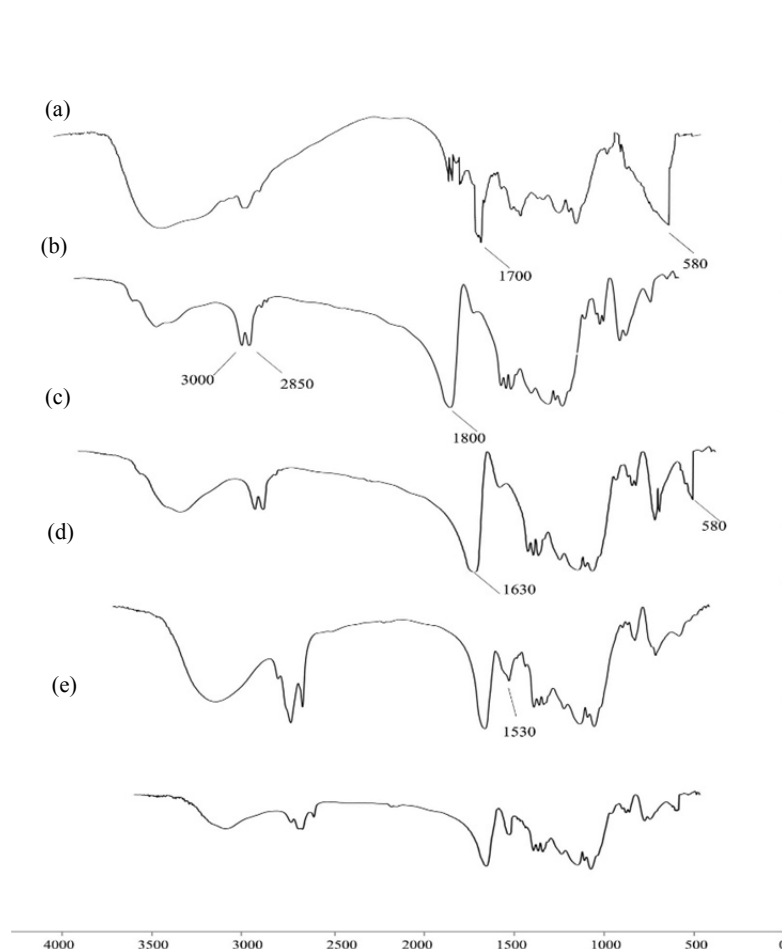
Fig. 4. FTIR spectrum of (a) magnetite nanoparticles, (b) oleic acid, (c) oleic acid-coated magnetite nanoparticles, (d) citric acid and (e) citric acid-coated magnetite nanoparticles.

(a)

(b)
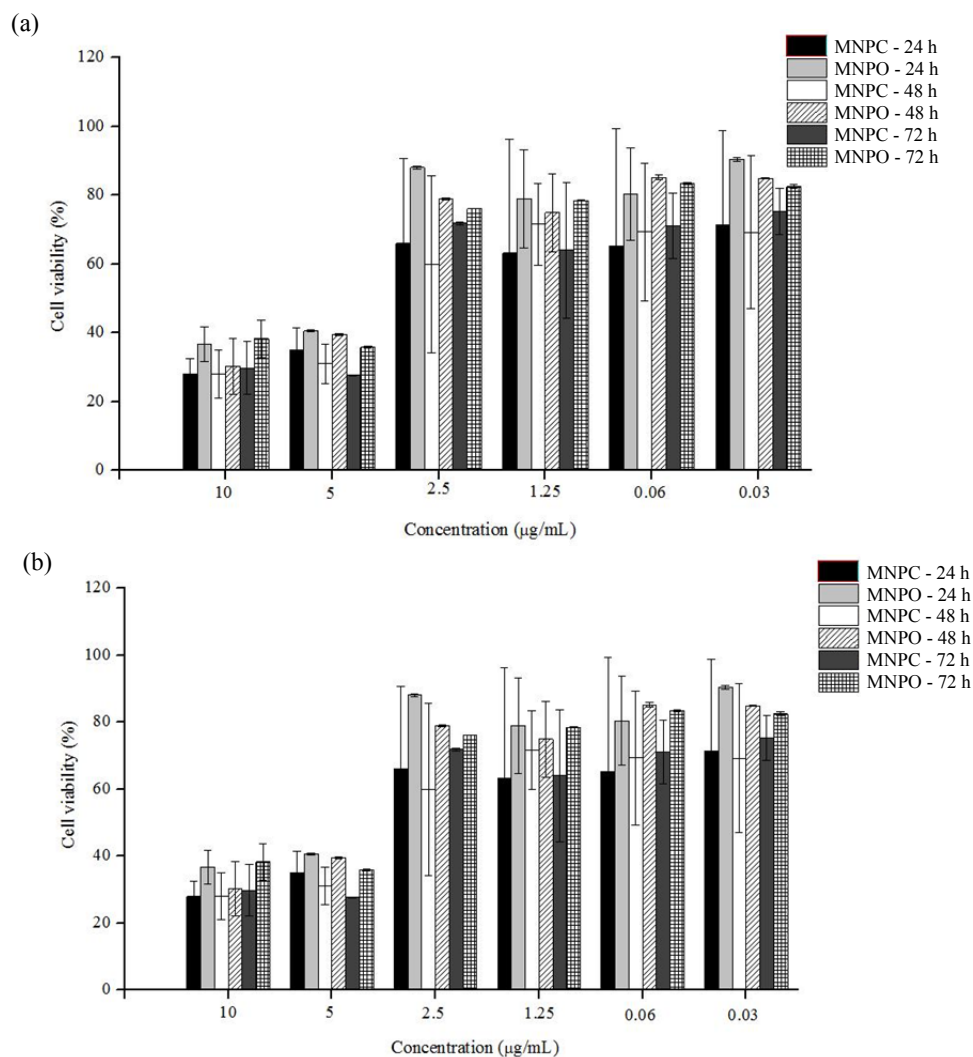
Fig. 5. (a) SK-Br-3, and (b) MCF-7 cell toxicity of oleic acid-coated magnetite nanoparticles and citric acid-coated magnetite nanoparticles over 24, 48 and 72 h.

DISCUSSION

MNPs known for their various capabilities in hyperthermia treatment, contrast enhancement agent and drug delivery carrier. However, finding optimum conditions to produce biologically relevant MNPs remains a challenge. To produce stable MNPs with small particle sizes, various conditions that affect the MNPs size, size distribution and stability were evaluated in detail in the current study.

At first the effect of mixing techniques on particle characteristics were examined. During mixing, it was found that the reported speed of 300 rpm or 600 rpm (13,14) is not sufficient to produce homogenous small particles. Although we attempted higher speeds, up to 1400 rpm, the desired size was not achieved.

This could be attributed to the attachment of the resulted MNPs to the stirrer bar, hampering the coating procedure and causing further aggregation of MNPs. Using bath sonication could not disperse particles efficiently. Under this situation, stabilizing agent may coat the aggregate of particles instead of single entities. Therefore, probe sonication was chosen as the alternative. Probe sonication with 100% intensity, resulted in particle sizes below 100 nm with narrow size distribution.

Mixing time of 30 min was determined to be the optimum time. Larger particles formed in 15 min, due to the incomplete reaction or lack of arrangement in the formed magnetite crystals, and in 45 min, due to crystal rearrangement and growth (Table 1). Time of mixing is also crucial for completion of

coating procedure. Consequently, the coating material was added when small crystals were formed and 30 min prior to their growth.

The source of iron also affects formation of MNPs and various salts could be used in this regard. We chose chloride salts due to their availability. Various iron salts ratio of 1.5, 1.75 or 2 have already been reported by different researchers (1,15,16). Using iron salts ratio of 2 resulted in smaller particles such as OMNPs-17 (70 nm). This is due to the reaction equilibrium that is reported to be 2 for Fe^{3+} to Fe^{2+} (17).

The media can be alkalinized using various alkalizing agents (13,18). When KOH or NaOH was used, the sizes of particles were as small as particles formed by ammonia but with higher polydispersity (Table 2). This may have caused by forming highly concentrated solutions with elevated pH that resembles longer reaction. Consequently, ammonia was employed as the alkalizing agent. The addition speed of ammonia also affected the particles. Faster addition of ammonia resulted in smaller MNPs (Table 2). This could be attributed to the prevention of crystal growth. Using stabilizing agents such as PVA or CMC resulted in sizes larger than OA or CA (Table 3). Both OA and CA deemed to be of similar sizes without any statistically significant differences. In stability studies, unlike naked MNPs that were aggregated, MNPs coated with OA or CA were stable.

Finally, freeze drying was selected for MNPs collection. The small and uniform size of acquired MNPs may be due to the reaction quenching and prevention of crystal growth at lower temperatures.

In TEM characterization, uncoated MNPs were aggregated (Fig. 1a). Meanwhile, OMNPs and CMNPs showed uniform, distinguishable and well-rounded surfaces (Fig. 1b, 1c). TEM measured particle sizes of 15 nm and 13 nm for OMNPs and CMNPs, respectively. The smaller sizes observed in TEM images compared to sizes measured by particle size analyzer may be due to the aggregation of two or more MNPs in solution or hydration of nanoparticles.

Magnetic saturation of naked MNPs was reported to be 90 emu/g which decreased to 60-65 emu/g as magnetically dead layer of OA covers its surface (14,16). Almost the same results were obtained by washing the magnetite nanoparticles with water (56 and 49 emu/g for OMNPs and CMNPs, graphs are not shown). Relatively higher MNPs saturation of 72 emu/g and 68 emu/g for OMNPs and CMNPs were obtained using the water and ethanol mixture (Fig. 2). That can be explained by extensive washing that removed excess OA or CA and only enough of stabilizer was present to retain surface stability.

X-ray powder diffraction (XRPD) spectrum (Fig. 3) was comparable with reported crystalline structure of magnetite (1). FTIR spectrum of naked MNPs (Fig. 4a) exhibited the absorption peak at 580-590 cm^{-1} that is attributed to Fe–O vibration (19). The broad peak in 3200-3600 cm^{-1} is attributed to hydroxyl group of water covering these charged particles. In OMNPs, the carboxyl vibration of OA is shifted to 1630cm^{-1} (Fig. 4c), due to its interaction with magnetite. In CMNPs the vibration of CA carboxyl group at 1780 cm^{-1} is absent (Fig. 4e), showing its chemical interaction with MNPs (20).

The dose response pattern of chosen MNPs, OMNPs-37 and CMNPs-39, were similar for both cell lines (Fig. 5). The results indicated that toxicity of OMNPs or CMNPs at low concentrations is negligible.

Upon further modification, synthesized MNPs have the potential to be used for theranostics for our long term goal of this research. Stealth coating of these MNPs is an ongoing work in our laboratory.

CONCLUSION

This study aimed at creating MNPs suitable for biological applications. MNPs were synthesized and the condition of production was optimized. MNPs of suitable sizes were characterized and imaged. Smallest particles were synthesized by 100% probe sonication intensity, iron salts ratio of 2 for 30 min, rapid ammonia addition, OA concentration of 0.2 mg/mL and freeze drying the particles. Suitable particle was resulted using CA and OA as stabilizing agent. Cell toxicity evaluation of these particles showed that at

low concentration their toxicity is negligible. In general, the designed system is suitable for biological applications due to its high magnetic saturation and low cytotoxicity.

REFERENCES

1. Lei Z, Li Y, Wei X. A facile two-step modifying process for preparation of poly(SStNa)-grafted Fe_3O_4/SiO_2 particles. J Solid State Chem. 2008;181(3):480–486.
2. Yildiz I, Yildiz BS. Applications of thermoresponsive magnetic nanoparticles. J Nanomater. 2015. Article ID 350596.
3. Pankhurst QA, Connolly J, Jones SK, Dobson J. Applications of magnetic nanoparticles in biomedicine. J Phys D: Appl Phys. 2003;36:R167–R181.
4. Cullity BD, Graham CD. Introduction to magnetic materials. 2nd ed: John Wiley&sons Inc. 2009. p. 87-114.
5. Lu AH, Salabas EL, Schüth F. Magnetic nanoparticles:synthesis, protection, functionalization, and application. Angew Chem Int Ed Engl. 2007;46(8):1222–1244.
6. Bogren S, Fornara A, Ludwig F, Morales MdP, Steinhoff U, Hansen MF, *et al*. Classification of magnetic nanoparticle systems—synthesis, standardization and analysis methods in the nanomag project. Int J Mol Sci. 2015;16(9):20308-20325.
7. McBain SC, Yiu HH, Dobson J. Magnetic nanoparticles for gene and drug delivery. Int J Nanomed. 2008;3(2):169-180.
8. Plank C, Schillinger U, Scherer F, Bergemann C, Rémy J-S, Krötz F, *et al*. The magnetofection method: using magnetic force to enhance gene delivery. Biol Chem. 2003;384(5):737-747.
9. Baryshev M, Vainauska D, Kozireva S, Karpovs A. New device for enhancement of liposomal magnetofection efficiency of cancer cells. World Acad Sci Eng Technol. 2011;58:249-252.
10. Mohammadi-Samani S, Miri R, Salmanpour M, Khalighian N, Sotoudeh S, Erfani N. Preparation and assessment of chitosan-coated superparamagnetic Fe_3O_4 nanoparticles for controlled delivery of methotrexate. Res Pharm Sci. 2013;8(1):25-33.
11. Alipour S, Montaseri H, Tafaghodi M. Inhalable, large porous PLGA microparticles loaded with paclitaxel:preparation, in vitro and in vivo characterization. J Microencapsul. 2015;32(7):661-668.
12. Park KS, Tae J, Choi B, Kim YS, Moon C, Kim SH, *et al*. Characterization, in vitro cytotoxicity assessment, and in vivo visualization of multimodal, RITC-labeled, silica-coated magnetic nanoparticles for labeling human cord blood–derived mesenchymal stem cells. Nanomedicine. 2010;6(2):263-276.
13. Chung TH, Pan HC, Lee WC. Preparation and application of magnetic poly(styrene-glycidyl methacrylate) microspheres. J Magn Magn Mater. 2007;311:36–40.
14. Chen YH, Liu YY, Lin RH, Yen FS. Characterization of magnetic poly(methyl methacrylate) microspheres prepared by the modified suspension polymerization. J Appl Polym Sci. 2008;108:583-590.
15. Ramirez LP, Landfester K. Magnetic polystyrene nanoparticles with a high magnetite content obtained by miniemulsion processes. Macromol Chem Physic. 2003;204(1):22-31.
16. Hong RY, Feng B, Cai X, Liu G, Li HZ, Ding J, *et al*. Double-miniemulsion preparation of Fe_3O_4/poly(methyl methacrylate) magnetic latex. J Appl Polym Sci. 2009;112(1):89-98.
17. R. Ahmadi, Madaah Hosseini HR, Masoudi A. Avrami behavior of magnetite nanoparticles formation In co-precipitation process. J Min Metall Sect B-Metall. 2011;47(2)B:211-218.
18. Mascolo MC, Pei Y, Ring TA. Room temperature co-precipitation synthesis of magnetite nanoparticles in a large pH window with different bases. Materials. 2013;6(12):5549-5567.
19. Hamoudeh M, Faraj AA, Canet-Soulas E, Bessueille F, Léonard D, Fessi H. Elaboration of PLLA-based superparamagnetic nanoparticles:characterization, magnetic behaviour study and in vitro relaxivity evaluation. Int J Pharm. 2007;338(1-2):248-257.
20. Pierre JL, Gautier-Luneau I. Iron and citric acid: A fuzzy chemistry of ubiquitous biological relevance. BioMetals. 2000;13(1):91-96.